Proceedings of Fifth International Conference on **Enhanced, Compact and Ultra-Compact Heat Exchangers: Science, Engineering and Technology**, Eds. R.K. Shah, M. Ishizuka, T.M. Rudy, and V.V. Wadekar, Engineering Conferences International, Hoboken, NJ, USA, September 2005.

CHE2005 – 09

STROUHAL NUMBERS AND POWER SPECTRUMS FOR TURBULENT FULLY-DEVELOPED FLOWS IN RECTANGULAR DUCTS WITH SPATIALLY-PERIODIC INTERRUPTED-PLATE INSERTS

Alexandre Lamoureux[*], Lorena Camargo[**], B. Rabi Baliga[***]

Department of Mechanical Engineering, Heat Transfer Laboratory, McGill University
817 Sherbrooke St. W., Montreal, Quebec H3A 2K6, Canada
[*]alexandre.lamoureux@mcgill.ca, [*]lorena.camargo@elf.mcgill.ca, [*]bantwal.baliga@mcgill.ca

ABSTRACT

An experimental study of fully developed flows of air in a straight rectangular duct with interrupted-plate inserts is presented. Values of the *dimensionless* geometric parameters, normalized with respect to the full height of the duct, are the following: width of the duct cross-section = 6.063; plate length = 1.001; plate thickness = 0.252 6; and inter-plate spacing = 1.004. The Reynolds number, based on average velocity at the minimum cross-sectional area and the hydraulic diameter, ranged from 2 000 to 30 000. Single hot-wire measurements and results, which include ensemble averaged power spectrums and Strouhal number distributions, are presented. They show repeatability, vertical and lateral symmetry at corresponding points in the central region of the duct cross-section, and spatial periodicity in successive geometrical modules.

INTRODUCTION

Industrial "micro" gas turbines (power range 25 kW to 500 kW) have been receiving increasing attention over the last decade as a viable power source for the distributed generation of electricity (McDonald, 2000). Thermal efficiencies in excess of 30% are essential to make these gas turbines economically and environmentally attractive for this application. Recuperators, that extract energy from the exhaust gas stream and heat the compressed air stream that is fed into the combustor, are used to achieve such high thermal efficiencies. These recuperators have compact cores (area-to-volume ratio > 700 m^2/m^3) with effectiveness usually exceeding 80% (McDonald, 2000).

In the cores of gas-turbine recuperators, primary-surface geometries with spatially periodic herringbone corrugations or interrupted-surface plate-fin flow passages are commonly used to enhance compactness and achieve excellent heat transfer-to-pumping power ratios (McDonald 2000; Kays and London, 1984). Discussions of fluid flows and the mechanisms responsible for enhancement of heat transfer in such interrupted-surface geometries are available in the works of London and Shah (1968), Sparrow et al. (1977), Cur and Sparrow (1979), Mullisen and Loehrke (1986), Mochizuki et al. (1987), Suzuki et al. (1994), Manglik and Bergles (1995), Zhang et al. (1997), DeJong et al. (1998), and Shah et al. (2001). Briefly, the interrupted surfaces repeatedly break and restart the velocity and thermal boundary layers, and also shed vortices for certain combinations of geometric parameters and Reynolds number, and these phenomena lead to high rates of heat transfer. However, they also produce pressure drops that are higher than those in plain or uninterrupted configurations. Thus, the design of interrupted-surface flow passages presents a thermofluid optimization problem, in which the objective is to achieve the highest possible rates of heat transfer for fixed pumping powers, over the full range of expected input conditions.

London and Shah (1968), Wieting (1975), and Kays and London (1984), have carried out experiments on full-scale models of compact heat exchangers, and they have proposed correlations for friction factor and Stanton number as a function of Reynolds number. Such works and correlations are useful in the design of specific heat exchangers. In the published literature, there are also numerous detailed experimental and numerical investigations of fluid flow and heat transfer in model geometries that are relevant to the design of compact heat exchangers with collinear and staggered parallel-plate arrays: Examples include the works of Sparrow et al. (1977), Patankar et al. (1977), Cur and Sparrow (1979), Joshi and Webb (1987), Mochizuki et al. (1987), McBrien and Baliga (1988), Manglik and Bergles (1995), Sebben and Baliga (1996), Acharya et al. (1997), Zhang et al. (1997), DeJong et al. (1998), Shah et al. (2001), and Candanedo et al. (2003). Such complementary detailed experimental and numerical investigations are essential for developing and refining the mathematical models and numerical methods

that are required for solving the aforementioned optimization problem.

Mathematical models and numerical methods for the simulation of steady and unsteady *laminar* flow and heat transfer in interrupted-surface geometries are pretty well established for essentially incompressible Newtonian fluids, as is seen, for example, in the works of Sparrow et al. (1977), Patankar et al. (1977), Amon et al. (1992), Suzuki et al. (1994), Grosse-Gorgemann et al. (1995), Zhang et al. (1997), Acharya et al. (1997), and DeJong et al. (1998). In the published literature, there are also numerous papers that report on attempts to simulate turbulent, incompressible, Newtonian fluid flows past bluff bodies and in interrupted-surface geometries. Reviews and details of such studies, and the associated issues, are available, for example, in the works of Wilcox (1993), Rodi et al. (1997), and Launder and Sandham (2002). Despite all of these efforts, however, the formulation of cost-effective mathematical models and numerical solution methods for the prediction of turbulent flows in interrupted-surface ducts continues to be a largely unattained goal, especially in the low-Reynolds number transitional and turbulent flow regimes, as discussed in Launder and Sandham (2002). The main aim of the work reported in this paper is to add to the repertoire of available experimental data that are suitable for testing and refining such mathematical models and numerical solution methods.

Some recent results of an ongoing complementary numerical and experimental investigation of flow and heat transfer through rectangular interrupted-surface ducts are presented in this paper. Attention is limited to single hot-wire measurements in the spatially-periodic regions of essentially isothermal (room temperature) flows of air through straight rectangular cross-section ducts with interrupted-plate inserts. Fast Fourier transforms of these hot-wire measurements are used to deduce ensemble averaged power spectrums (one-sided power spectral densities) and Strouhal numbers. Numerous studies involving hot-wire and laser-Doppler measurements of velocity and turbulence quantities for single cylinders (of both circular and square cross-section) in essentially unconfined cross flows are available in the literature. Reviews and examples of such studies are available in the works of Norberg (1994), Lyn et al. (1995), Williamson (1996), and Rodi et al. (1997). However, there are essentially no papers that present detailed turbulence measurements in the spatially-periodic regions of flows in interrupted-surface ducts, even though such measurements are urgently needed. This paper attempts to fulfill a small part of this need.

A schematic illustration of the duct used in this work is given in Fig. 1. Though this duct is relatively simple geometrically, the flow through it exhibits complexities similar those that characterize flows in the cores of plate-fin compact heat exchangers (Kays and London, 1984), namely, periodic interruptions of the shear layers on the interrupted plates and vortex shedding for certain
combinations of the geometric parameters and Reynolds numbers. Static pressure distributions and heat transfer measurements for flows in similar ducts have been reported by Cur and Sparrow (1979), McBrien and Baliga (1988), Amon et al. (1992), Grosse-Gorgemann et al. (1995), and Candanedo et al. (2003). The single hot-wire measurements reported in this paper complement the static pressure distributions reported by Candanedo et al. (2003).

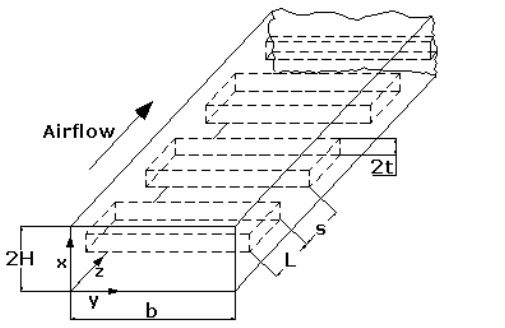

Figure 1: Schematic illustration of a straight duct of rectangular cross-section with interrupted-plate inserts.

NOMENCLATURE

$A_{c-s-min}$	Minimum cross-sectional area [Eq. (2)]
A_{wetted}	Wetted surface area [Eq. (2)]
b	Channel width [Fig. 1]
D_h	Hydraulic diameter [Eq. (2)]
f	Frequency [Hz]
f_v	Frequency of the primary (first) spike in the PSD_m results [Hz]
$H(f)$	Fourier transform of v' [Eq. (6)]
H, L, s, t	Duct half-height, plate length, inter-plate spacing, half-thickness of plate [Fig. 1]
L^*, s^*, t^*	Dimensionless plate length, inter-plate spacing, and plate thickness [Eq. (1)]
$\dot{m}$	Mass flow rate of air
$\tilde{p}(x,y,z)$	Spatially periodic part of time-mean static pressure distribution [Eq. (4)]
$P(x, y, z)$	Time-mean static pressure
PSD_m	Power spectrum (one-sided power spectral density) ensemble averaged over 100 blocks of data [Eq. (6)]
Re	Reynolds number [Eq. (1)]
U, V, W	Time-mean x-, y-, and z-direction velocity components at any point (x, y, z)
v	Magnitude of instantaneous cross flow velocity experienced by the hot wire
$\bar{v}, v'$	Time-mean value of v and $(v-\bar{v})$
$\bar{W}$	Cross-sectional average W [Eq. (2)]
x,y,z	Cartesian coordinates [Figs. 1 and 4]
β	Time-mean overall pressure drop per unit length in the duct [Eq. (4)]
$\varepsilon, \varepsilon_{Rel}$	Roughness (*rms* value) and ε/D_h
λ	Aspect ratio of duct cross-section [$b/2H$]
Λ	Spatial period ($L+s$)

μ Dynamic viscosity of air
ρ Mass density of air

EXPERIMENTAL APPARATUS AND PROCEDURES

Overview

The experimental facility used in this work is schematically presented in Figure 2. It consists of the following main elements: (i) a test section in which the wall static pressure distributions can be measured; (ii) a flow visualization section where the hot-wire measurements were made; (iii) a flow transition section; (iv) a flow metering section; (v) a flow control, generation, and exhaust section; and (vi) a data acquisition and processing system. Details of these elements are concisely presented in this section. Additional details are available in the work of Candanedo et al. (2003).

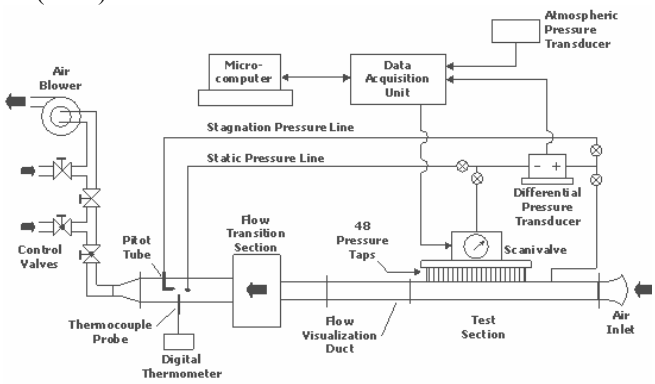

Figure 2: Schematic of the overall experimental setup.

Test and Flow Visualization Sections

The test and flow visualization sections, are both straight rectangular cross-section ducts, which can be configured with and without interrupted-plate inserts. The walls of the test section are made of aluminum, while those of the flow visualization section are made of clear acrylic (Lexan). The dimensional and dimensionless geometrical details of these sections are given in Table 1, in terms of the notations provided in Fig. 1.

The aspect ratio, λ, used in this work ensures essentially two-dimensional flow over the central region of the duct cross-section. The values of L^* and s^* are representative of those found in compact heat exchangers (Kays and London, 1984). The value of t^* used here is more than double that found in Kays and London (1984): this was done in order to accentuate the vortex shedding phenomenon. The objective here was to obtain accurate experimental measurements that would be useful in testing and refining of methods for computer simulations of time-periodic, low-Reynolds number, transitional and turbulent flows in interrupted-surface geometries, rather than data that are directly applicable to the design of compact heat exchangers. The total length of the test section is 152 4 mm, which allowed this portion of the flow passage to be configured with 30 geometrically similar modules, each of length ($L + s$) in the main flow direction (z in Fig. 1). The length of the flow visualization section is 609.6 mm, which allowed another 12 geometrically symmetric modules (contiguous with those in the test section) to be included in the flow circuit. Thus, spatially periodic fully-developed flow could be expected to prevail over at least the last 18 modules in the test section and all modules in the flow visualization section (Sparrow et al., 1977; Cur and Sparrow, 1979; Candanedo et al., 2003). The interrupted-plates were made of precision-ground steel and had sharp square edges.

Table 1: Cross-sectional and modular dimensions of the test and flow visualization sections. The uncertainties in b, $2H$, L, $2t$, and s are all less than ± 0.03 mm.

b [mm]	$2H$ [mm]	L [mm]	$2t$ [mm]	s [mm]
152.67	25.18	25.21	6.36	25.59

D_h [mm]	$\lambda = b/2H$	$L^* = L/2H$	$t^* = 2t/2H$	$s^* = s/2H$
21.32	6.063	1.001	0.252 6	1.004

The top plate of the flow visualization section was designed with a total of nine holes through which a special jig for holding the single hot-wire probe could be inserted (see Fig. 3). This set-up allowed the single hot-wire to be oriented normal to the main flow direction (z) and parallel to the y direction at 12 different positions (see Fig. 4) in each of three different longitudinal cross-sections of the duct, in the space between the interrupted plates.

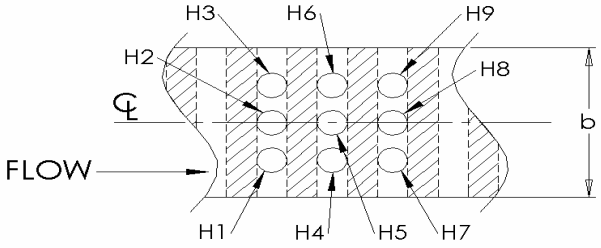

Figure 3: Holes in the top plate of the flow visualization section for the insertion of a jig to hold the single hot-wire probe. The shaded regions are top views of the plates.

The x-z coordinates of the hot-wire positions in Fig. 4, with respect to the origin of the axes shown in this figure, are given in Table 2. The centers of holes H2, H5, and H8 are in the central longitudinal cross-section of the duct, while those of holes H3, H6, and H9, and H1, H4, and H7, are each shifted off laterally from the longitudinal centerline by 38.1 mm [Fig. 3].

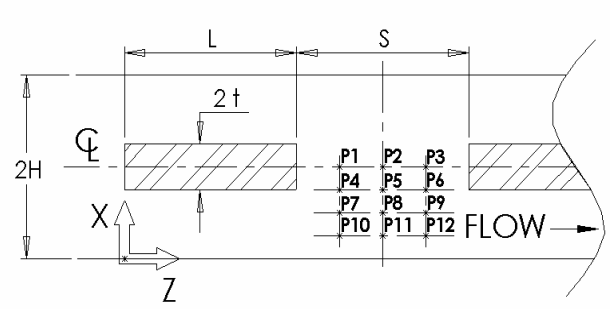

Figure 4: Positions of the single hot-wire probe in the longitudinal cross-section of the duct.

Table 2: Coordinates of the hot-wire positions (in mm) in each longitudinal cross-section of the duct, with reference to the local *x*-*z* axes shown in Fig. 4. The uncertainties in these positions are all less than ± 0.10 mm.

	P1	**P2**	**P3**	**P4**	**P5**	**P6**
x	12.5	12.5	12.5	9.3	9.3	9.3
z	32.4	39.2	46.1	32.4	39.2	46.1

	P7	**P8**	**P9**	**P10**	**P11**	**P12**
x	6.1	6.1	6.1	3.0	3.0	3.0
z	32.4	39.2	46.1	32.3	39.2	46.1

Hot-Wire Instrumentation

The hot-wire anemometer used in this study was a DISA CTA Bridge 56C16 (with overheat ratio of 1.825). A single hot-wire probe was used (TSI 1210 – T1.5). This probe is made of platinum coated tungsten wire. The platinum is etched out in the sensing region: wire diameter 3.81 x 10^{-3} mm and length 1.27 mm. This hot-wire probe was calibrated often during the experiments (typically, every week). The ambient air temperature during the calibration procedures *and* the actual experimental runs was 23.3 °C ± 0.5 °C. The hot-wire data acquisition and processing procedures are described in the next subsection.

Data Acquisition Procedures

The hot-wire signals were acquired using a personal computer, a National Instruments PCI-6036E A/D card, and a BNC–2110 board. The sampling frequency was fixed at 10 000 Hz, the gain was set to one (unity), and low-pass filtering at 10 000 Hz was used. The hot-wire data was acquired using programs written in Lab View, in blocks of 8192 samples. In each case (each flow), 100 such blocks of data were acquired and stored. Later, for each flow, this data was processed as follows: the data for each block was processed to obtain fast Fourier transforms (fft) and power spectrums (one-sided power spectral density distributions); and the power spectrums for the 100 blocks of data were then ensemble averaged.

Benchmarking

The experimental facilities, instrumentation, and procedures for measuring pressures and overall flow rates have been carefully benchmarked and reported by Candanedo et al. (2003). The hot-wire system was benchmarked by measuring the frequency of vortex shedding from a cylinder of circular cross-section in essentially uniform cross flow. This experiment was conducted in a wind tunnel with a test section cross-section of 1 m x 1m. The aspect ratio (length to diameter ratio) of this cylinder was greater than 30, and the Reynolds number was varied in the range 1 000 – 20 000. The results (Strouhal number versus Reynolds number) were all well within the usual scatter exhibited by available results, as discussed in Norberg (1994) and Williamson (1996).

THEORETICAL CONSIDERATIONS AND DATA REDUCTION

The dimensionless parameters that characterize the turbulent flows investigated here are the following:

$$Re = \rho \bar{W} D_h / \mu \;\; ; \;\; \lambda = b/(2H) \;\; ; \;\; L^* = L/(2H)$$
$$s^* = s/(2H) \;\; ; \;\; t^* = 2t/(2H) = t/H \;\; ; \;\; \varepsilon_{Rel} = \varepsilon / D_h \qquad (1)$$

In this work, the wetted surfaces of the test and flow visualization sections were all smooth (the *rms* roughness, ε, on all these surfaces was well less than the viscous sublayer thickness in all cases), so the effect of ε/D_h on the flow could be considered negligible. The definitions of D_h and $\bar{W}$ given by Kays and London (1984) were used. Thus, with respect to the notation given in Fig. 1:

$$\Lambda = L + s \;\; ; \;\; A_{c-s-min} = 2b(H-t)$$
$$A_{wetted} = 2[(2L+s)b + 2\{L(H-t) + Hs\} + 2bt] \qquad (2)$$
$$D_h = 4A_{c-s-min}\Lambda / A_{wetted} \;\; ; \;\; \bar{W} = \dot{m}/(\rho A_{c-s-min})$$

In interrupted-plate rectangular ducts akin to that shown in Fig. 1, spatially periodic fully-developed turbulent flow is characterized by *time-mean* *x*-, *y*-, and *z*-direction velocity components (*U*, *V*, and *W*, respectively) that repeat identically in geometrically similar modules. Thus, denoting the spatial period by $\Lambda = (L + s)$, the following equation applies:

$$U(x,y,z) = U(x,y,z+\Lambda) = U(x,y,z+2\Lambda) = \ldots$$
$$V(x,y,z) = V(x,y,z+\Lambda) = V(x,y,z+2\Lambda) = \ldots \qquad (3)$$
$$W(x,y,z) = W(x,y,z+\Lambda) = W(x,y,z+2\Lambda) = \ldots$$

Following Patankar et al. (1977), for spatially periodic fully developed flows, the variation of the *time-mean* static pressure can be expressed by the following equation:

$$P(x,y,z) = -\beta z + \tilde{p}(x,y,z) \qquad (4)$$

The term $-\beta z$ is related to the overall mass flow rate in the duct, and $\tilde{p}(x,y,z)$ is spatially periodic in the z direction. Thus, with reference to Fig. 1,

$$\tilde{p}(x,y,z) = \tilde{p}(x,y,z+\Lambda) = \tilde{p}(x,y,z+2\Lambda) = \ldots \qquad (5)$$

As was stated earlier, single hot-wire measurements were used to obtain power spectrums and the variation of Strouhal number with Reynolds number for the flows of interest in this work. The single hot-wire was maintained perpendicular to the main flow direction (z) and parallel to the y direction (Fig. 1). Let $v(x,y,z,t)$, $\bar{v}(x,y,z)$, and $v'(x,y,z,t)$ denote the magnitude of the instantaneous cross flow velocity, its time-mean value, and its fluctuation about this mean value, respectively, experienced by this single hot-wire probe at any particular spatial location (x,y,z) in the duct. Then,

$$v = \bar{v} + v' \; ; \; H(f) = \int_{-\infty}^{\infty} v'(t) e^{-2\pi i f t} dt$$
$$PSD_m(f) = \left[\sum_{block=1}^{100} \frac{2}{\Delta t_{block}} | H_{block}(f) |^2 \right] / 100 \qquad (6)$$

Here, f is the frequency (in *Hz*), Δt_{block} is the total time needed to obtain samples in *each* block of hot-wire data (each block of data consisting of 8192 samples taken at 10,000 *Hz*), $H(f)$ is the Fourier transform of $v'(x,y,z,t)$, and $PSD_m(f)$ is the power spectrum (one-sided power spectrum density) ensemble averaged over the 100 block of data. Fast Fourier transforms and Hann data windowing were used. Details are available in Press et al. (1992).

RESULTS AND DISCUSSION

Uncertainties, Repeatability, Symmetry, and Spatial Periodicity

The methods elaborated by Moffat (1985) were used to estimate uncertainties in the experimental results. In all cases considered here, the uncertainties in the reported values of the Reynolds number, Re, and the ensemble averaged power spectrums, $PSD_m(f)$, were estimated to be less than ±2% and ±3%, respectively.

Numerous initial tests were done to establish the repeatability (for similar experimental runs), the symmetry (at corresponding symmetrical vertical and lateral points in the cross-section of the duct), and the spatial periodicity (at corresponding positions in successive geometrically similar modules of the duct) of the power spectrums and Strouhal number distributions. For any given flow rate, these measurements and results were repeatable within the implicit experimental uncertainties. A sample of such repeatability checks is given Fig. 5.

The symmetry of the hot-wire measurements at corresponding vertical positions in the cross-section of the duct is well represented by the results given in Fig. 6. These results also establish that the blockage effects of the single hot-wire probe are negligibly small.

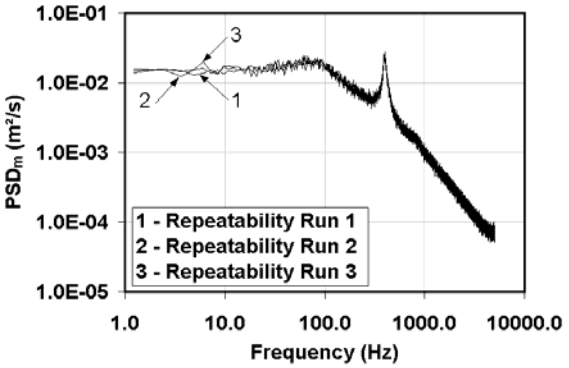

Figure 5: Repeatability of ensemble averaged power spectrums (PSD_m) at position P8 (Fig. 4, Table 2), hole H2 (Fig. 3): results for Re ≈ 20 000.

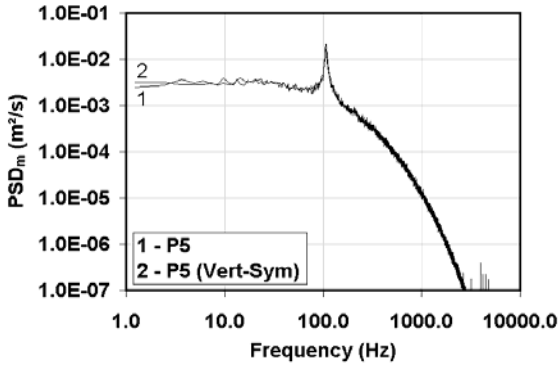

Figure 6: Ensemble averaged power spectrums (PSD_m) at position P5 (Fig. 4, Table 2), hole H2 (Fig. 3) and its vertically symmetrical position: results for Re ≈ 5 000.

On the top plate of the flow visualization section, the holes for the insertion of the hot-wire support jig (Fig. 3) have their centers spaced 38.1 mm apart in the y direction (see Fig. 1) direction. Numerous initial measurements showed that the ensemble averaged features of the flows considered here are essentially two-dimensional over at least the central 76.2 mm in the lateral direction of the duct cross-section: see the sample results shown in Fig. 7.

As was mentioned earlier in this paper, spatially periodic fully-developed flow was expected to prevail over at least the last 15 modules in the test section and all modules in the flow visualization section. Initial tests confirmed that this expectation was indeed met, as shown by the samples results presented in Fig. 8.

Earlier experimental works have also established the occurrence of the spatially periodic regime for flows in interrupted-surface ducts, but based on time-mean heat transfer data and wall static pressure measurements: see, for example, the works Cur and Sparrow (1979), Joshi and Webb (1987), McBrien and Baliga (1988), Manglik and Bergles (1995), and Candanedo et al. (2003). However, this is first time that it has been experimentally shown that turbulence statistics, such as ensemble averaged PSD_m, also display spatially periodic behavior in such flows.

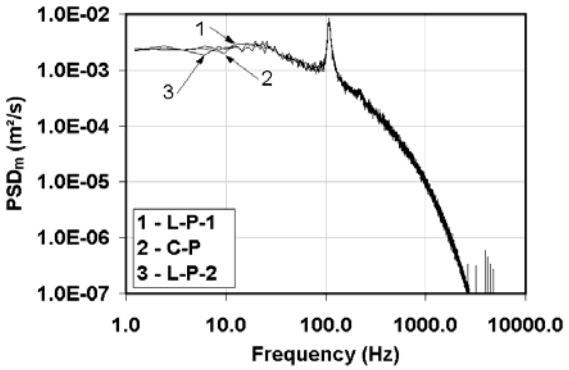

Figure 7: Ensemble averaged power spectrums (PSD_m) at position P8 in holes H4 (L-P-1), H5 (C-P), and H6 (L-P-2) [see Figs. 3 and 4]: results for Re ≈ 5 000.

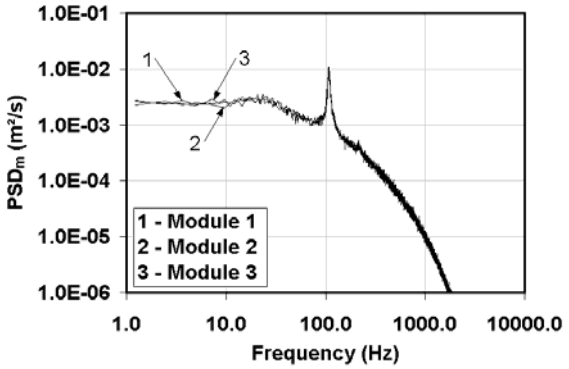

Figure 8: Ensemble averaged power spectrums (PSD_m) at position P8 [Fig. 4] in successive geometrical modules of the duct in the flow visualization section [holes H2, H5, and H8; Fig. 3]: results for Re ≈ 5 000.

Ensemble Averaged Power Spectrums

Ensemble averaged power spectrums (one-sided power spectral density) were obtained for all 12 of the hot-wire positions shown in Fig. 4, for hole H5 (Fig. 3), for Reynolds number [Eq. (1)] in the nominal range 2 000 – 30 000. Sample PSD_m results for positions P1, P2, P7, and P8 are given in Figs. 9(a) – 9(d), respectively.

In the gaps between successive interrupted plates, the flow is both temporally and spatially complex, with possible direct interactions between four separated shear layers (from the leading and trailing edges on the bottom and top surfaces of the interrupted plates) and the boundary layers on the top, bottom, and side walls of the duct. Despite these possible interactions, the single hot-wire measurements established that ensemble averaged features of these flows are essentially two-dimensional over at least the central 76.2 mm in the lateral direction of the duct cross-section, as was discussed earlier in this paper (see Fig. 7).

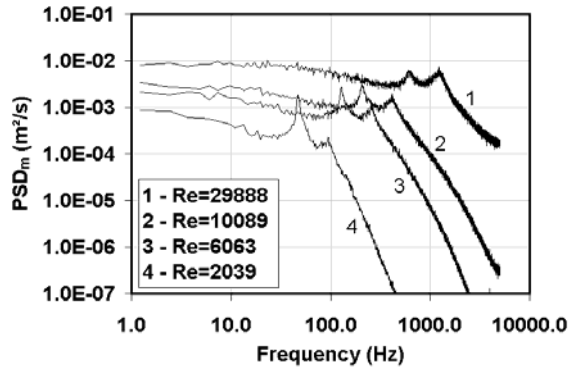

(a)

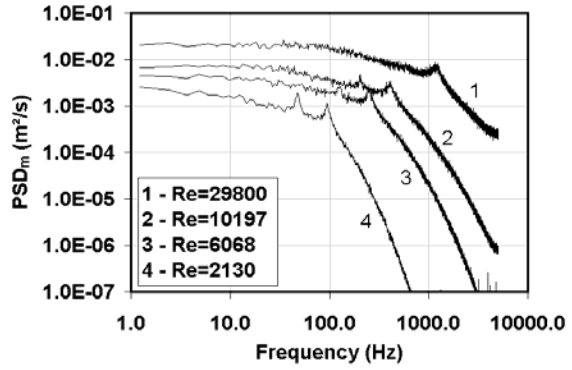

(b)

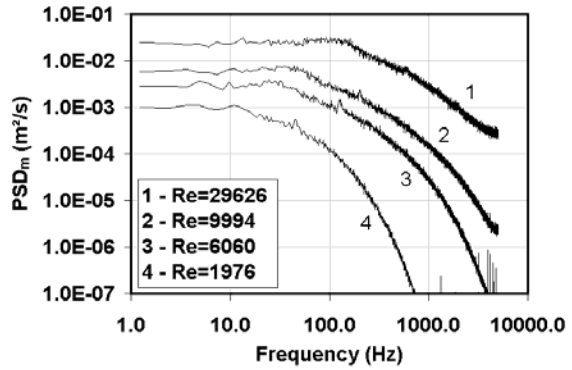

(c)

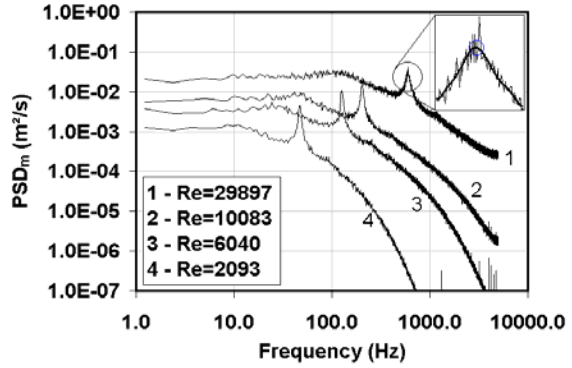

(d)

Figure 9: PSD_m) results (hole *H5*): (a) position P1, (b) position P2, (c) position P7, and (d) position P8.

The ensemble averaged PSD_m results illustrate that there are strongly time-periodic flow phenomena in the wake region of the plates in the duct. In Figs. 9(a) and 9(b), the PDS_m results clearly show two spikes, with the frequency of the second spike essentially double that of the first one, establishing that counter-rotating vortices are shed alternately from the top and bottom trailing edges of the interrupted plates. In the PSD_m results presented in Figs. 9(c) and 9(d), only one prominent spike is evident, showing that at hot-wire positions P7 and P8, the influence of the vortices shed from the top edge of the interrupted plate is negligible.

Strouhal Numbers

The frequency corresponding to the first spike in the PSD_m results [for example, in Figs. 9(a)], or the single spike in these results [for example, in Fig. 9(d)], is referred to here as the primary frequency, and denoted as f_v. This frequency was determined by using a least-squares fit of a ninth-order polynomial to a sufficient number of data points (that adequately capture the spike of interest in the PSD_m), and deducing the frequency that gives the local maximum in this polynomial. Such a curve fit to the spike in the PSD_m is schematically illustrated in the inset in Fig. 9(d). This primary frequency is expressed in dimensionless terms as the Strouhal number:

$$St = f_v(2t)/\overline{W} \tag{7}$$

Over the particular positions P1 – P12 (Fig. 4), the time-periodic phenomena in the gaps between the interrupted plates are narrow-banded rather than monochromatic, with respect to both spatial location and the Reynolds number. The corresponding Strouhal numbers are given in Table 3.

CONCLUSION

An experimental study of fully-developed flows of air in a straight rectangular duct with interrupted-plate inserts has been presented in this paper. The focus was on single hot-wire measurements. The results, which include ensemble averaged power spectrums and Strouhal number distributions, show repeatability, vertical and lateral symmetry at corresponding points in the central region of the duct cross-section, and spatial periodicity in successive geometrical modules. This is first time that it has been experimentally established that turbulence statistics, such as ensemble averaged power spectrums (PSD_m), and also Strouhal number distributions display spatially periodic behavior. The results presented here would be useful as checks on mathematical models and numerical solution methods for computer simulations of turbulent flows in interrupted-surface passages akin to those encountered in compact heat exchangers.

Table 3: Variation of Strouhal number with position and Reynolds number (N/A indicates that is no discernable time-periodic phenomenon).

P1		P4		P7		P10	
Re	***St***	***Re***	***St***	***Re***	***St***	***Re***	***St***
2 039	0.203	2 039	0.204	1 976	N/A	1 937	N/A
3 015	0.198	3 007	0.196	3 045	0.197	2 962	N/A
3 995	0.195	3 987	0.194	4 057	N/A	4 036	N/A
5 063	0.190	4 992	0.190	4 973	0.189	5 010	N/A
6 063	0.186	5 956	0.187	6 060	N/A	5 997	N/A
8 075	0.184	8 146	0.182	8 079	N/A	8 044	N/A
10 088	0.180	10 089	0.179	9 994	N/A	9 926	N/A
20 078	0.174	20 127	0.175	20 099	N/A	20 034	N/A
29 888	0.177	29 645	0.177	29 626	N/A	29 770	N/A

P2		P5		P8		P11	
Re	***St***	***Re***	***St***	***Re***	***St***	***Re***	***St***
2 130	0.200	1 976	0.202	2 093	0.200	1 984	0.205
2 982	0.198	3 018	0.198	3 027	0.197	3 069	0.196
4 066	0.189	4 082	0.192	4 114	0.192	4 087	0.190
4 983	0.188	5 145	0.187	5 160	0.187	5 049	0.188
6 069	0.183	5 996	0.186	6 040	0.186	6 072	0.183
8 055	0.181	8 070	0.182	8 160	0.181	8 155	0.181
10 197	0.178	10 026	0.179	10 083	0.179	10 000	0.178
20 218	N/A	20 003	0.173	20 239	0.174	20 075	0.174
29 800	N/A	29 799	0.174	29 897	0.173	29 722	0.173

P3		P6		P9		P12	
Re	***St***	***Re***	***St***	***Re***	***St***	***Re***	***St***
2 026	0.206	2 061	0.198	1 992	0.200	1 960	0.202
3 022	N/A	3 012	N/A	3 069	0.194	2 971	0.196
4 010	N/A	3 994	N/A	4 058	0.190	4 035	0.191
5 097	N/A	4 979	N/A	4 965	0.187	5 011	0.186
6 043	N/A	5 957	N/A	6 052	0.184	6 057	0.184
8 074	N/A	8 138	0.177	8 089	0.179	8 019	0.181
10 082	N/A	10 064	0.172	9 977	0.177	9 946	0.178
20 053	N/A	20 108	0.169	20 037	0.172	20 079	0.174
29 786	N/A	29 541	0.169	29 499	0.173	29 721	0.172

ACKNOWLEDGEMENTS

Financial support of the Natural Sciences and Engineering Research Council of Canada (NSERC), in the form of postgraduate scholarships to the first and second authors and research grants to the third author, is gratefully acknowledged. The authors would also like to express their thanks to Professor L. Mydlarski and Mr. Etienne Costa-Patry for their invaluable advice and help with the hot-wire measurements.

REFERENCES

Acharya, S., Myrum, T., Sinha, S., and Qiu, X., 1997, Developing and Periodically Developed Flow, Temperature and Heat Transfer in a Ribbed Duct, *Int. J. Heat Mass Transfer*, Vol. 40, pp. 461-480.

Amon, C.H., Majumdar, D., Herman, C.V., Mayinger, F., Mikic, B.B., and Sekulic, D., 1992, Numerical and Experimental Studies of Self-Sustained Oscillatory Flows in Communicating Channels, *Int. J. Heat Mass Transfer*, Vol. 35, pp. 3115-3129.

Candanedo, J.A., Aboumansour, E., and Baliga, B.R., 2003, Time-Mean Wall Static Pressure Distributions and Module Friction Factors for Fully Developed Flows in a Rectangular Duct with Spatially Periodic Interrupted-Plate Inserts, *Proc. ASME International Mechanical Engineering Congress & Exposition (IMECE 2003)*, Nov. 16-21, Washington, D.C., pp. 1-10.

Cur, N., and Sparrow, E.M., 1979, Measurements of Developing and Fully Developed Heat Transfer Coefficients Along a Periodically Interrupted Surface, *ASME J. Heat Transfer*, Vol. 101, pp. 211-216.

DeJong, N.C., Zhang, L.W., Jacobi, A.M., Balachandar, S., and Tafti, D.K., 1998, A Complementary Experimental and Numerical Study of the Flow and Heat Transfer in Offset Strip-Fin Heat Exchangers, *ASME J. Heat Transfer*, Vol. 120, pp. 690-698.

Grosse-Gorgemann, A., Weber, D., Fiebig, M., 1995, Experimental and Numerical Investigation of Self-Sustained Oscillations in Channels with Periodic Structures, *Expt. Thermal and Fluid Sc.*, Vol. 11, pp. 226-233.

Joshi, H.M., and Webb, R.L., 1987, Heat Transfer and Friction in the Offset Strip-Fin Heat Exchanger, *Int. J. Heat Mass Transfer*, Vol. 30, pp. 69-84.

Kays, W.M., and London, A.L., 1984, *Compact Heat Exchangers*, 3rd ed., McGraw-Hill, New York.

Launder, B.E., and Sandham, N.D. (eds.), 2002, Introduction, in *Closure Strategies for Turbulent and Transitional Flows*, Cambridge Univ. Press, U.K.

London, A.L., and Shah, R.K., 1968, Offset Rectangular Plate-Fin Surfaces – Heat Transfer and Flow Friction Characteristics, *ASME J. Eng. Power*, pp. 218-228.

Lyn, D.A., Einav, S., Rodi, W., Park, J.-H., 1995, A Laser-Doppler Velocimetry Study of Ensemble-Average Characteristics of the Turbulent Near Wake of a Square Cylinder, *J. Fluid Mech.*, Vol. 304, pp. 285-319.

Manglik, R.M., and Bergles, A.E., 1995, Heat Transfer and Pressure Drop Correlations for the Rectangular Offset Strip Fin Compact Heat Exchanger, *Expt. Thermal and Fluid Sc.*, Vol. 10, pp. 171-180.

McBrien, R.K., and Baliga, B.R., 1988, Module Friction Factors and Intramodular Pressure Distributions for Periodic Fully Developed Turbulent Flow in Rectangular Interrupted-Plate Ducts, *ASME J. Fluids Eng.*, Vol. 110, pp. 147-154.

McDonald, C.F., 2000, Low Cost Recuperator Concept for Microturbine Applications, *Proceedings of ASME TURBOEXPO 2000, Paper No. 2000-GT-167,* Munich, Germany, May 8-11.

Mochizuki, S., Yagi, Y., and Yang, W.-J., 1987, Transport Phenomena in Stacks of Interrupted Parallel-Plate Surfaces, *Expt. Heat Transfer*, Vol. 1, pp. 127-140.

Moffat, R.J., 1985, Using Uncertainty Analysis in the Planning of an Experiment, *ASME J. of Fluids Eng.*, Vol. 107, pp. 173-182.

Mullisen, R.S., and Loehrke, R.I., 1986, A Study of the Flow Mechanisms Responsible for Heat Transfer Enhancements in Interrupted-Plate Heat Exchangers, *ASME J. Heat Transfer*, Vol. 108, pp. 377-385.

Norberg, C., 1994, An Experimental Investigation of the Flow Around a Circular Cylinder: Influence of Aspect ration, *J. Fluid Mech.*, Vol. 258, pp. 287-316.

Patankar, S.V., Lui, C.H., and Sparrow, E.M., 1977, Fully Developed Flow and Heat Transfer in Ducts Having Streamwise-Periodic Variation of Cross-Sectional Area, *ASME J. Heat Transfer*, Vol. 99, pp. 180-186.

Press, L., Teulosky, S.A., Vetterling, W.T., and Flannery, B.P., 1992, *Numerical Recipes in FORTRAN: The Art of Scientific Computing*, 2nd ed., Cambridge Univ. Press, U.K.

Rodi, W., Ferziger, J.H., Breuer, M., and Pourquié, M., 1997, Status of Large-Eddy Simulation: Results of a Workshop, *ASME J. Fluids Eng.*, Vol. 119, pp. 248-262.

Sebben, S., and Baliga, B.R., 1996, Turbulent Flow in Periodic Interrupted-Surface Passages, *Proc. Brazilian Congress of Engineering & Thermal Sciences*, Florianopolis, Brazil, Nov. 11-14, pp. 1815-1820.

Shah, R.K., Heikal, M.R., Thonon, B., and Tochonp, P., 2001, Progress in Numerical Analysis of Compact Heat Exchanger Surfaces, in *Advances in Heat Transfer*, Vol. 34, pp. 363-443.

Sparrow, E.M., Baliga, B.R., and Patankar, S.V. 1977, Heat Transfer and Fluid Flow Analysis of Interrupted-Wall Channels, With Application to Heat Exchangers, *ASME J. Heat Transfer*, Vol. 99, pp. 4-11.

Suzuki, K., Xi, G.N., Inaoka, K., and Hagiwara, Y., 1994, Mechanism of Heat Transfer Enhancement Due to Self-Sustained Oscillation for an In-Line Fin Array, *Int. J. Heat Mass Transfer*, Vol. 37, Suppl. 1, pp. 83-96.

Wieting, A.R., 1975, Empirical Correlations for Heat Transfer and Flow Friction Characteristics of Rectangular Offset-Fin Plate-Fin Heat Exchangers, *ASME J. Heat Transfer*, Vol. 97, pp. 488-490.

Williamson, C.H.K., 1996, Vortex Dynamics in the Cylinder Wake, *Annu. Rev. Fluid Mech.*, Vol. 28, pp. 477-539.

Wilcox, D.C., 1993, *Turbulence Modelling for CFD*, DCW Industries Inc., La Cañada, California, U.S.A.

Zhang, L.W., Balachandar, S., Tafti, D.K., and Najjar, F.M., 1997, Heat Transfer Enhancement Mechanisms in Inline and Staggered Parallel-Plate Fin Heat Exchangers, *Int. J. Heat Mass Transfer*, Vol. 40, pp. 2307-2325.